Available online at www.sciencedirect.com
ScienceDirect
Nuclear Instruments and Methods in Physics Research A 580 (2007) 1588–1593
NUCLEAR INSTRUMENTS & METHODS IN PHYSICS RESEARCH Section A
www.elsevier.com/locate/nima

Analysis of interface states and series resistance at MIS structure irradiated under ^{60}Co γ-rays

A. Tataroğlu*, Ş. Altındal

Department of Physics, Faculty of Arts and Sciences, Gazi University, 06500 Ankara, Turkey

Received 24 April 2007; received in revised form 3 July 2007; accepted 17 July 2007
Available online 22 July 2007

Abstract

In this research, we investigated the effect of ^{60}Co γ-ray exposure on the electrical properties of Au/SnO_2/n-Si (MIS) structures using current–voltage (I–V) measurements. The fabricated devices were exposed to γ-ray doses ranging from 0 to 300 kGy at a dose rate of 2.12 kGy h^{-1} in water at room temperature. The density of interface states N_{ss} as a function of E_c–E_{ss} is deduced from the forward bias I–V data for each dose by taking into account the bias dependence effective barrier height and series resistance of device at room temperature. Experimental results show that the γ-irradiation gives rise to an increase in the zero bias barrier height Φ_{BO}, as the ideality factor n and N_{ss} decrease with increasing radiation dose. In addition, the values of series resistance were determined using Cheung's method. The R_s increases with increasing radiation dose. The results show that the main effect of the radiation is the generation of interface states with energy level within the forbidden band gap at the insulator/semiconductor interface.

PACS: 73.20.At; 73.30.+y; 73.40.Sx; 84.37.+q; 61.80.−x; 73.20.−r

Keywords: γ-Ray effects; MIS structures; I–V characteristics; Interface states; Series resistance

1. Introduction

Metal–insulator–semiconductor (MIS) and metal–oxide–semiconductor (MOS) structures consist of a semiconductor substrate covered by an insulator layer upon which a metal electrode is deposited. The presence of the insulating interface layer makes them rather sensitive to irradiation. It is known that energetic ^{60}Co γ-irradiation can generate electronic surface states at the semiconductor–insulator (such as Si–SnO_2 or Si–SiO_2) interface in MIS structures. The high-level particles such as proton, neutron, electron and γ-ray irradiation at the interface cause modification of the interface and affect the electrical characteristics of the MIS structure formed on the semiconductor. These defects act as recombination centers trapping the generated carriers. Therefore, it is interesting to investigate the effects of the defect centers on the performance of these devices. Further, the development of radiation resistance MIS and MOS structures is necessary for widespread applications. Recently, the radiation response of MIS structures has been found to change significantly when these structures are exposed to irradiation stress treatments [1–13].

Da Silva et al. [11], Winokur et al. [6] and Ma [2,4] were among the first to make a systematic observation of the after-irradiation behavior of interband radiation-induced interface states (N_{ss}) at the semiconductor–insulator interface in MIS structures. Especially there are two important effects of radiation to be considered: (a) the transient effects due to the electron–hole pair generation and (b) permanent effect due to the bombardment of devices with radiation, causing changes in the crystal lattice. The radiation-generated holes may diffuse in the insulator, but are less mobile than the electrons; many stationary holes traps are also present.

SnO_2 thin films have been one of the most important metal oxides due to their properties and potential applications. The superior chemical stability of SnO_2 thin films and their promising physical properties have motivated

*Corresponding author. Tel.: +90 312 2126030; fax: +90 312 2122279.
E-mail address: ademt@gazi.edu.tr (A. Tataroğlu).

0168-9002/$ - see front matter © 2007 Elsevier B.V. All rights reserved.
doi:10.1016/j.nima.2007.07.027

their application in many devices, such as solar cells, gas sensors, catalyses devices, metallurgy, biotechnology, nuclear technology and transparent conducting electrodes [14–16].

In order to achieve a better understanding of the effect of ^{60}Co γ-ray irradiation on the electrical characteristics of Au/SnO_2/n-Si MIS structures, we measured both forward- and reverse bias current–voltage (I–V) characteristics as a function of dose rate at room temperature. The structures are stressed with a zero bias during γ-ray irradiation with the dose rate of 2.12 kGy h^{-1} in water and total dose range was 0–300 kGy. After each dose, we present the changes in electrical characteristics evaluated using forward and reverse bias I–V measurements. Before and after each dose, the density of N_{ss} profiles as a function of E_c–E_{ss} was extracted from the forward bias I–V characteristics. In addition, experimental results for the diodes are compared with results published for these type of semiconductor devices.

2. Experimental detail

The MIS (Au/SnO_2/n-Si) structures used in this work were fabricated using n-type (P-doped) single crystal silicon wafers with ⟨1 1 1⟩ surface orientation, 300 μm thickness, 2″ diameter and 1 Ω cm resistivity. The Si wafer was degreased for 5 min in boiling trichloroethylene, acetone and ethanol consecutively and then etched in: first H_2SO_4, H_2O_2 and 20% HF solution, then $6HNO_3$:1HF:$35H_2O$ and 20% HF solution. Preceding each cleaning step, the wafer was rinsed thoroughly in de-ionized water of 18 MΩ cm resistivity. Immediately after surface cleaning, high-purity Au metal (99.999%) with a thickness of 2500 Å was thermally evaporated from the tungsten filament onto the whole back surface of the wafer in liquid nitrogen trapped oil-free ultra-high vacuum system in the pressure of 1×10^{-6} Torr. The ohmic contacts were prepared by sintering the evaporated back contact at about 700 °C for 20 min in flowing dry nitrogen (N_2) ambient at rate of 1.5 l min^{-1}. This process served to sinter the Au on surface of n-type Si wafer. Immediately after ohmic contact, a thin layer of SnO_2 was grown on the n-Si substrate by spraying a solution consisting of 32.21 wt% of ethyl alcohol (C_2H_5OH), 40.35 wt% of de-ionized water (H_2O) and 27.44 wt% of stannic chloride ($SnCl_4\cdot5H_2O$) on the substrate, which was maintained at a constant temperature of 400 °C. The temperature of the substrates was monitored by chromel–alumel thermocouple fixed on top surface of the substrate. The variation of the substrate temperature during spray was maintained within ±2 °C with the help of a temperature controller. The rate of spraying was kept at about 30 cc min^{-1} by controlling the carrier gas flow-meter. N_2 was used as the carrier gas. SnO_2 dots were 4 mm in diameter. After spraying process, circular dots of 1 mm in diameter and 2500 Å thick Au rectifying contacts were deposited onto the SnO_2 surface of the wafer through a metal shadow mask in liquid nitrogen trapped oil-free ultra-high vacuum system in the pressure of 1×10^{-6} Torr. Both the thickness of metal layer and deposition rates were monitored with the help of a digital quartz crystal thickness monitor. The deposition rates were about 1–3 Å s^{-1}. The interfacial oxide layer thickness was estimated to be about 66 Å from measurement of the oxide capacitance in the strong accumulation region for MIS structure.

The I–V measurements were carried out using a Keithly 220 programmable constant-current source and a Keithly 614 electrometer. The fabricated Au/SnO_2/n-Si MIS structure was exposed to ^{60}Co γ-radiation of doses ranging from 50 to 300 kGy at a dose rate of 2.12 kGy h^{-1} in water at room temperature. The electrical properties of the structure were analyzed before and after radiation exposure. All measurements were carried out with the help of a microcomputer through an IEEE-488 ac/dc converter card.

3. Results and discussion

According to the thermionic emission (TE) theory for a MIS Schottky diode with series resistance the relation between an applied forward bias ($V\geqslant3kT/q$) and current can be written as [17,18]

$$I = I_o \exp\left(\frac{q(V-IR_s)}{nkT}\right)\left[1-\exp\left(\frac{-q(V-IR_s)}{kT}\right)\right] \quad (1)$$

where the IR_s term is the voltage drop across series resistance of structure, I_o the saturation current derived from the ln(I)–V plot as the straight line intercept of the ln(I) axis at zero bias, V the applied voltage across to rectifier contact, n the ideality factor, T the absolute temperature in K, q is the electronic charge and k is the Boltzmann constant. Due to the existence of series resistance (R_s), a significant voltage drop occurs at large forward currents. This amounts to the reduction of the voltage across the barrier region, metal–semiconductor interface, from the actually applied to the terminals of the MIS structure. In this case, the ln(I)–V plot deviates from a straight line at high forward bias. The ideality factor n is introduced to take into account the deviation of the experimental I–V data from the ideal thermionic model, and the value of ideality factor should be one for an ideal contact. The saturation current I_o is given by

$$I_o = AA^*T^2\exp\left(-\frac{q\Phi_{BO}}{kT}\right) \quad (2)$$

where A is the diode area, A^* is the effective Richardson constant of 120 A cm^{-2} K^{-2} for n-type Si [18] and Φ_{BO} ($kT/q\ln[AA^*T^2/I_o]$) is the zero bias barrier height. The ideality factor is a measure of the conformity of the diode current to be pure TE, and it is calculated from the slope of the linear region of the forward bias ln(I)–V plot according to

$$n = \frac{q}{kT}\frac{d(V-IR_s)}{d(\ln I)} \quad (3a)$$

where $d(V–IR_s)/d(\ln I)$ is the slope of linear region of $\ln(I)–V$ plots. Also the voltage-dependent ideality factor $n(V)$ can be written from Eq. (1) as

$$n(V) = \frac{q}{kT}\frac{(V - IR_s)}{\ln(I/I_o)} \tag{3b}$$

One of the most widely used methods to measure the Schottky barrier heights, series resistance and interface states was the forward bias $I–V$ measurements technique. Therefore, we obtained a typical forward and reverse bias semi-logarithmic $I–V$ characteristics of the MIS structure before and after γ-ray irradiation at room temperature and are given in Fig. 1. As can be seen in Fig. 1, each plot consists of a good linear range with different slopes in intermediate bias regions. The reverse saturation current I_o is determined from the intercept of forward bias $\ln(I)–V$ plot on the y-axis at zero bias for each dose rate. Putting these values of I_o in Eq. (2), the values of Schottky barrier heights Φ_{BO} are evaluated. As can be seen from Fig. 1, the value of the reverse current was observed to decrease with increase in the radiation dose up to a level of 300 kGy, whereas the effect of irradiation on the forward bias current was almost negligibly low. Specifically, the reverse current (at −3 V) decreased from 22.60 μA (before irradiation) to 1.50 μA (300 kGy), whereas the forward bias current (at 3 V) decreased from 1.66 mA (before irradiation) to 0.72 mA (300 kGy). This radiation-induced enhancement observed in the reverse bias $I–V$ characteristics could be attributed to the decrease in interfacial defect density, unlike in Ref. [8]. Such behavior of the reverse bias $I–V$ characteristics was observed by Kinoshita et al. [10]. They show that the leakage currents increase with γ-dose up to the range 0.4–1.5 MGy and decrease with γ doses above 1.5 MGy.

The variations in both ideality factor and barrier height as a function of radiation dose are given in Fig. 2 and Table 1, respectively. As can be seen in Fig. 2 and Table 1, the ideality factor n exhibits a decreasing trend with increasing dose. Before irradiation the ideality factor n was found to be 2.370. After irradiation, the ideality factor changes from 2.206 (at 50 kGy) to 1.796 (at 300 kGy). These behaviors of the ideality factor suggest that the current transport mechanism consists of both the trap-assisted tunneling and the TE [17]. In addition, the decrease in reverse current can be attributed to irradiation-induced defects at the MS interface that enhances the defect-assisted tunneling. Similar results have been commonly observed in $I–V$ measurements of MIS structure and they are attributed to the presence of a thin insulating layer between the metal and semiconductor. The image-force effect, recombination-generation and tunneling may be other possible mechanisms that could lead to an ideality factor value greater than unity [9,19–23].

The values of zero bias barrier height ($\Phi_{BO} = \Phi_B$) were obtained from intercepts of the forward bias $\ln(I)–V$ plot for each irradiation dose (Fig. 2). As can be seen in Fig. 2, the values of Φ_B increase exponentially with increase radiation dose. In this case, the unirradiated diode has a barrier height of 0.744 eV. However, after irradiation, the experimental values of barrier height change from 0.753 (at 50 kGy) to 0.799 (at 300 kGy). The results account for a net reduction in carrier density in the depletion region of MIS structure through the occurrence of traps and recombination centers associated with radiation damage [9,21,22].

The interface states for electrons or holes must not necessarily introduce energy levels in the band gap, i.e., only the density of states in the valence and conduction bands may be affected. The non-linearity of $I–V$ characteristics of the MIS structure at high bias values indicates a continuum of interface states, which are in equilibrium

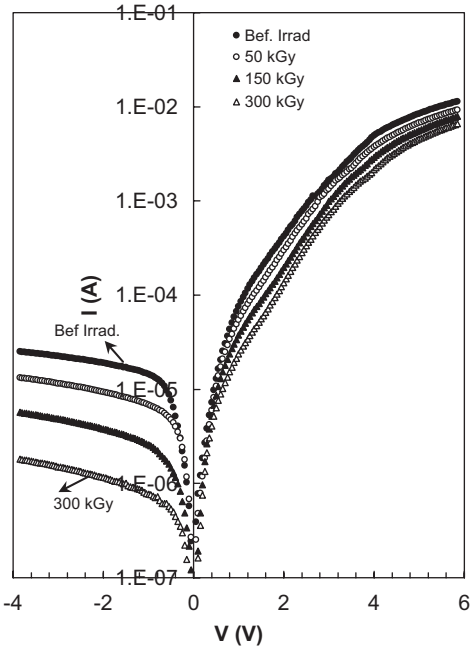

Fig. 1. Forward and reverse bias $I–V$ characteristics of $Au/SnO_2/n$-Si (MIS) structure before and after γ-ray irradiation.

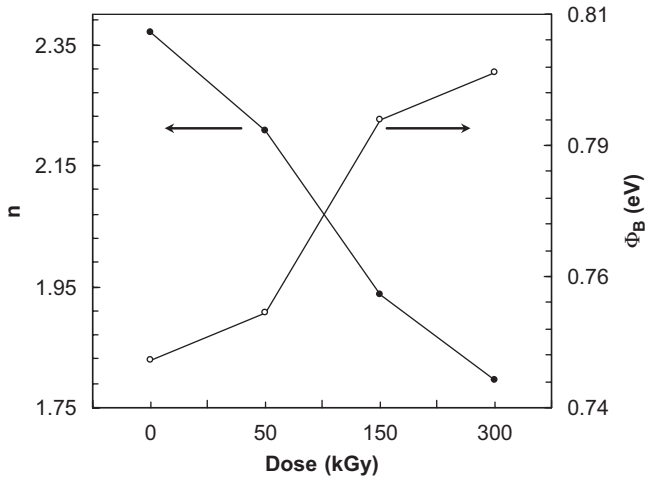

Fig. 2. Variation of ideality factor and barrier height as a function of γ-ray dose for the MIS structure.

Table 1
Radiation dependency of various parameters determined from forward bias I–V characteristics of Au/SnO_2/n-Si (MIS) structure

Irradiation (kGy)	I_o (A)	N	Φ_{BO} (eV)	R_s ($dV/d(\ln I)$) (Ω)	R_s ($H(I)$) (Ω)	W_D (cm)	N_{ss} ($eV^{-1}cm^{-2}$)
Bef. Irrad.	1.03×10^{-7}	2.370	0.744	285.87	277.88	3.05×10^{-4}	8.02×10^{12}
50	7.22×10^{-8}	2.206	0.753	337.08	322.00	2.83×10^{-4}	7.05×10^{12}
150	1.77×10^{-8}	1.938	0.790	370.09	361.26	2.58×10^{-4}	5.48×10^{12}
300	1.22×10^{-8}	1.796	0.799	417.87	406.03	2.24×10^{-4}	4.64×10^{12}

with the semiconductor [24]. Nevertheless, the structures exhibit excellent rectification characteristics with a relatively low-leakage current density. The effective barrier height Φ_e is assumed to be bias dependent due to the presence of an interfacial insulator layer and interface states located at the SnO_2/Si interface. The applied voltage dependence of the barrier height can be written as

$$\frac{d\Phi_e}{dV} = \beta = 1 - \frac{1}{n(V)} \tag{4}$$

where β is the voltage coefficient of the effective barrier height Φ_e and is given by [23–26]

$$\Phi_e = \Phi_{BO} + \beta(V - IR_s) = \Phi_{BO} + (1 - \frac{1}{n(V)})(V - IR_s). \tag{5}$$

The Φ_e is a parameter that includes the effects of both interface states in equilibrium with the semiconductor [24] and series resistance. For MIS Schottky diodes having interface states N_{ss} in equilibrium with semiconductor, the ideality factor n is given by

$$n(V) = 1 + \frac{\delta}{\varepsilon_i}\left[\frac{\varepsilon_s}{W_D} + qN_{ss}(V)\right] \tag{6a}$$

where ε_i and ε_s are the permittivity of the insulator layer (SnO_2) and the semiconductor, respectively, and W_D is width of the depletion region. This expression of voltage-dependent ideality factor is identical to Eq. (18) of Card and Rhoderick [24]. The expression for the interface state density as deduced by Card and Schroder [24,27] is reduced to [17,28]

$$N_{ss}(V) = \frac{1}{q}\left[\frac{\varepsilon_i}{\delta}(n(V) - 1) - \frac{\varepsilon_s}{W_D}\right] \tag{6b}$$

where δ is the thickness of the interfacial insulator layer. The other parameters are defined as before. The thickness δ can be obtained for the MIS Schottky diode from sufficiently high frequency ($f \geqslant 500$ kHz) C–V measurements using the equation $C_i = \varepsilon_i\varepsilon_0 A/\delta$, where C_i is the capacitance of the interfacial insulator layer (SnO_2) [18,29] and ε_0 is the permittivity of free space. The depletion layer width being deduced from the experimental C–V measurements at high frequency is given by [18]

$$W_D = \sqrt{\frac{2\varepsilon_s}{qN_D}\psi_s} \tag{7}$$

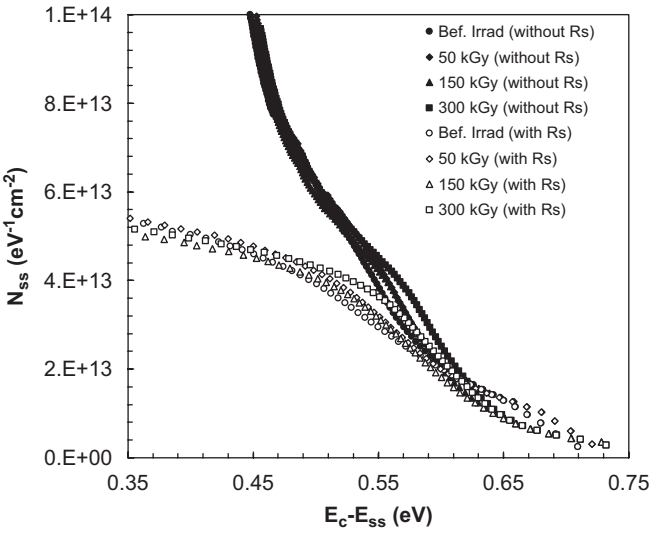

Fig. 3. The density of interface states (N_{ss}) distribution profiles as a function E_c–E_{ss} obtained from the forward bias I–V characteristics for each dose.

where ψ_s is the surface potential and N_D is the carrier concentration. Furthermore, in n-type semiconductors, the energy of interface states E_{ss} with respect to the bottom of the conduction band, E_c, at the surface of semiconductor is given by [24,25,30]

$$E_c - E_{ss} = q(\Phi_e - V). \tag{8}$$

When MIS or MOS structures are exposed to ionizing radiation, additional interface states, called "radiation-induced interface states", can be generated at the insulator/semiconductor such as SiO_2/Si and SnO_2/Si interface. Therefore, for each radiation dose, the density of N_{ss} distribution profiles as a function of E_c–E_{ss} were obtained from the forward bias I–V characteristics taking into account Φ_e with and without R_s by substituting the values of voltage-dependent $n(V)$, $\varepsilon_s = 11.8\varepsilon_0$, $\varepsilon_i = 7\varepsilon_0$ and $\delta = 66$ Å, in Eq. (6b).

Fig. 3 shows the density of interface states (N_{ss}) distribution profiles as a function E_c–E_{ss} for each dose was extracted from the forward bias I–V characteristics taking into account both the bias dependence of the effective barrier height and with and without taking into account R_s obtained from the forward bias I–V characteristics of the MIS structure for each dose at room temperature. The exponential increase of the N_{ss} from the

mid-gap toward the bottom of the conductance band is very apparent [4,9,10,21,31,32]. In addition, the density of interface states decreases with increasing radiation dose, being attributed to the decrease in recombination center and the existence of an interfacial insulator layer (SnO_2) at MIS interface.

As seen in Fig. 3, the magnitude of the N_{ss} with and without the R_s at $E_c = -0.46$ eV is in the range 8.29×10^{13} to $4.40 \times 10^{13}\,eV^{-1}\,cm^{-2}$ (before irradiation) and at the same E_c value it is in the range 9.10×10^{13} to $4.63 \times 10^{13}\,eV^{-1}\,cm^{-2}$ (300 kGy). The values of N_{ss} obtained taking into account the R_s are lower than those obtained without considering the R_s. The above explanations clearly show that the R_s value should be taken into account in determining the interface state density distribution profiles.

Therefore, the series resistance R_s values were also determined from the functions developed by Cheung and Cheung [33]. The Cheung's functions

$$\frac{dV}{d(\ln I)} = IR_s + n\left(\frac{kT}{q}\right) \tag{9}$$

which should be a straight line for the data of downward curvature region of the forward bias I–V measurements.

$$H(I) = V - n\left(\frac{kT}{q}\right)\ln\left(\frac{I}{AA^*T^2}\right) = n\Phi_B + IR_s \tag{10}$$

where Φ_B is the barrier height obtained from intercept of $H(I)$ vs. I plots. The term IR_s is the voltage drop across the series resistance of MIS structure. In Fig. 4(a) and (b), the experimental $dV/d\ln(I)$ vs. I and $H(I)$ vs. I plots are presented at different irradiation doses for the MIS structure, respectively. Thus, the slope and y-axis intercept of the plot $dV/d\ln(I)$ vs. I will give R_s and nkT/q, respectively. As a function of radiation, the values of R_s were derived from Fig. 4(a) and (b). The plots associated with these functions are given in Fig. 4(a). The series resistance values were determined from Eq. (9). A plot of $H(I)$ vs. I according to Eq. (10) will also give a straight line with the y-axis intercept equal to $n\Phi_B$. The plots associated with these functions are given in Fig. 4(b). Here, the series resistance values were determined from Eq. (10).

The slope of this plot also provides the second determination of R_s, which can be used to check the consistency of Cheung's approach. The values of series resistance calculated from Eqs. (9) and (10) for each irradiation dose are presented in Table 1. As can be seen in Table 1, the values of R_s obtained from $dV/d(\ln I)$–I and $H(I)$–I plots are in good agreement with each other and increase strongly with increasing irradiation [5,9,21,34]. The effect of the series resistance R_s is usually modeled with a series combination of a diode and a resistor with resistance R_s, through which the current flows. Such behavior of the R_s can be explained as being due to changes in the effective dopant density due to carrier removal by the defects produced [35].

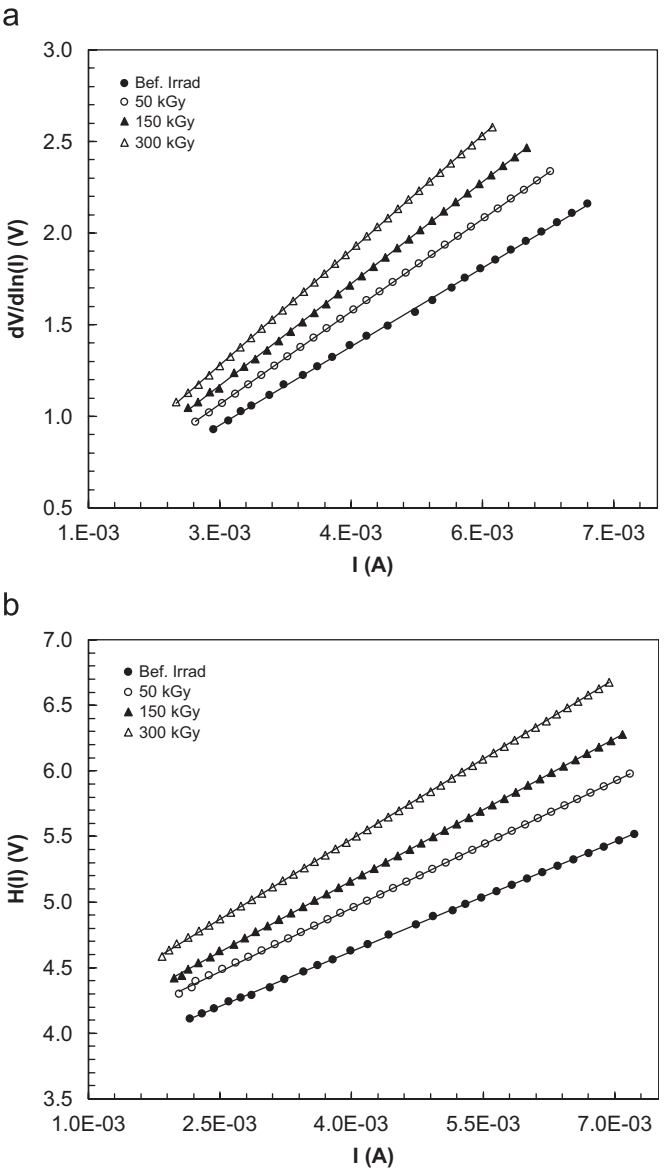

Fig. 4. (a) Experimental $dV/d\ln(I)$ vs. I and (b) $H(I)$ vs. I plots for the MIS structure at different irradiation doses.

4. Conclusion

$Au/SnO_2/n$-Si (MIS) structures were exposed to ^{60}Co γ-ray radiation of doses ranging from 0 to 300 kGy, and the effect of γ-irradiation on the current–voltage (I–V) characteristics was analyzed before and after exposure to radiation at room temperature. The ideality factor (n) values obtained from I–V characteristics are higher than unity, and this is attributed to the presence of a thin insulating layer between the metal and semiconductor. Exposure to increasing cumulative γ-ray doses was found to have the following main affects: (a) an apparent increase in zero bias barrier height Φ_{BO} and series resistance R_s; (b) significant degradation in reverse bias I–V characteristics; and (c) an apparent decrease in ideality factor n and density of interface states N_{ss}. The variation of the reverse current

could be due to creation of a radiation defect, which compensates the positive charges at the insulator/semiconductor interface and consequently leads to a reduction in the electrical parameters. In other words, the decrease of the reverse bias I–V characteristics could be attributed to a decrease in interfacial defect density. After the γ-ray radiation, a decrease in the ideality factors is especially true in diodes with the current density of dislocations which are exposed to increasing doses of energy irradiation, because any radiation-induced changes within the dislocation-free area of the insulator–semiconductor interface may not manifest in the forward bias I–V characteristics. The density of interface states (N_{ss}) decreases with increasing radiation dose, being attributed to the decrease in the recombination centers and the passivation of the Si surface due to the deposition insulator layer (SnO_2).

Acknowledgments

This work is partly supported by Turkish of Prime Ministry State Planning Organization Project no. 2001K120590.

References

[1] T.R. Oldham, Ionizing Radiation Effects in MOS Oxides, World Scientific Publishing, Singapore, 1999.
[2] T.P. Ma, P.V. Dressendorfer, Ionizing Radiation Effect in MOS Devices and Circuits, Wiley, New York, 1989.
[3] M.R. Chin, T.P. Ma, Appl. Phys. Lett. 42 (10) (1983) 883.
[4] T.P. Ma, Semicond. Sci. Technol. 4 (1989) 1061.
[5] M.Y. Feteha, M. Soliman, N.G. Gomaa, M. Ashry, Renew. Energy 26 (2002) 113.
[6] P.S. Winokur, J.M. McGarrity, H.E. Boesch, IEEE Trans. Nucl. Sci. NS-23 (1976) 1580.
[7] S. Kaschieva, Zh. Todorova, S.N. Dmitriev, Vacuum 76 (2004) 307.
[8] G.A. Umana-Membreno, J.M. Dell, G. Parish, B.D. Nener, L. Faraone, U.K. Mishra, IEEE Trans. Electron. Devices ED-50 (12) (2003) 2326.
[9] A. Tataroğlu, Ş. Altındal, M.M. Bülbül, Nucl. Instr. and Meth. A 568 (2) (2006) 863.
[10] A. Kinoshita, M. Iwami, K. Kobayashi, I. Nakano, R. Tanaka, T. Kamiya, A. Ohi, T. Ohshima, Y. Fukushima, Nucl. Instr. and Meth. A 541 (2005) 213.
[11] E.F. Da Silva Jr., Y. Nishioka, T.P. Ma, IEEE Trans. Nucl. Sci. NS-34 (6) (1987) 1190.
[12] K.H. Zainninger, A.G. Holmes-Siedle, RCA Rev. (1967) 208.
[13] K. Naruke, M. Yoshida, K. Maegushi, H. Tango, IEEE Trans. Nucl. Sci. NS-30 (6) (1983) 4054.
[14] D.B. Chrisey, G.K. Hubler, Pulsed Laser Deposition of Thin Films, Wiley, New York, 1994.
[15] O. Auciello, J. Engemann, Multicomponent and Multilayered Thin Films for Advanced Microtechnologies: Techniques Fundamentals and Devices, Kluwer, Dordrecht, 1993.
[16] W. Dazhi, W. Shulin, C. Jun, Z. Suyuan, L. Fangqing, Phys. Rev. B 49 (1994) 14282.
[17] E.H. Rhoderick, R.H. Williams, Metal-Semiconductor Contacts, second ed., Clarendon Press, Oxford, 1988.
[18] S.M. Sze, Physics of Semiconductor Devices, second ed., Wiley, New York, 1981.
[19] A. Goetzberger, V. Heine, E.H. Nicollian, Appl. Phys. Lett. 12 (1968) 95.
[20] G.W. Hughes, J. Appl. Phys. 48 (12) (1977) 5357.
[21] Ş. Karataş, A. Türüt, Ş. Altındal, Nucl. Instr. and Meth. A 555 (1–2) (2005) 260.
[22] R. Khanna, K. Ip, K.K. Allums, K. Baik, C.R. Abernathy, S.J. Pearton, Y.W. Heo, D.P. Norton, F. Ren, R. Dwivedi, T.N. Fogarty, R. Wilkins, Phys. Status Solidi A 201 (12) (2004) R79.
[23] P. Chattopadhyay, A.N. Daw, Solid State Electron. 29 (5) (1986) 555.
[24] H.C. Card, E.H. Rhoderick, J. Phys. D 4 (1971) 1589.
[25] A. Singh, K.C. Reinhardt, W.A. Anderson, J. Appl. Phys. 68 (7) (1990) 3478.
[26] P. Cova, A. Singh, Solid State Electron. 33 (1) (1990) 11.
[27] D.K. Schroder, Semiconductor Material and Device Characterization, Wiley, London, 1998.
[28] E.H. Nicollian, A. Goetzberger, Appl. Phys. Lett. 7 (1965) 216.
[29] E.H. Nicollian, J.R. Brews, MOS Physics and Technology, Wiley, New York, 1982.
[30] M.K. Hudait, S.B. Krupanidhi, Mater. Sci. Eng., B 87 (2001) 141.
[31] J.M. Benedetto, H.E. Boesch Jr., IEEE Trans. Nucl. Sci. NS-31 (6) (1984) 1461.
[32] G.W. Hughes, J. Appl. Phys. 48 (12) (1977) 5357.
[33] S.K. Cheung, N.W. Cheung, Appl. Phys. Lett. 49 (2) (1986) 85.
[34] S. Kar, K.M. Panchal, S. Bhattacharya, S. Varma, IEEE Trans. Electron. Devices ED-29 (1982) 1839.
[35] R.D. Harris, A.J. Frasca, IEEE Trans. Nucl. Sci. NS-53 (2006) 1995.